

An intrinsically disordered yeast prion arrests the cell cycle by sequestering a spindle pole body component

Sebastian Treusch^{1,2} and Susan Lindquist^{1,2}

¹Whitehead Institute for Biomedical Research, Cambridge, MA 02142

²Howard Hughes Medical Institute, Department of Biology, Massachusetts Institute of Technology, Cambridge, MA 02139

Intrinsically disordered proteins play causative roles in many human diseases. Their overexpression is toxic in many organisms, but the causes of toxicity are opaque. In this paper, we exploit yeast technologies to determine the root of toxicity for one such protein, the yeast prion Rnq1. This protein is profoundly toxic when overexpressed but only in cells carrying the endogenous Rnq1 protein in its [RNQ⁺] prion (amyloid) conformation. Surprisingly, toxicity was not caused by general proteotoxic stress. Rather, it involved a highly specific mitotic arrest mediated by the Mad2 cell cycle

checkpoint. Monopolar spindles accumulated as a result of defective duplication of the yeast centrosome (spindle pole body [SPB]). This arose from selective Rnq1-mediated sequestration of the core SPB component Spc42 in the insoluble protein deposit (IPOD). Rnq1 does not normally participate in spindle pole dynamics, but it does assemble at the IPOD when aggregated. Our work illustrates how the promiscuous interactions of an intrinsically disordered protein can produce highly specific cellular toxicities through illicit, yet highly specific, interactions with the proteome.

Introduction

Proteins with intrinsically disordered regions (IDRs) are of intense interest, as they are broadly toxic in diverse organisms when their expression is elevated (Vavouri et al., 2009) and feature in many protein misfolding diseases (Stefani and Dobson, 2003). Intrinsically disordered proteins often form amyloids, β sheet-rich fibrous structures (Chiti and Dobson, 2006). Amyloid formation is associated with many human diseases (Ross and Poirier, 2005), yet it is no longer thought to be the primary source of toxicity in most of these diseases (Kayed et al., 2003; Treusch et al., 2009). Rather, it is the propensity of intrinsically disordered forms of amyloidogenic proteins to accumulate as soluble oligomers and amorphous aggregates that enables their gain-of-function toxicities.

The complex biology of proteins with IDRs has made the nature of their toxicities difficult to decipher. Their common gene dosage-related toxicity likely arises from detrimental, mass action-driven promiscuous protein-protein interactions (Vavouri et al., 2009). The toxicity of artificial β sheet proteins,

for example, seems to result from their interactions with disordered proteins that occupy essential hub positions in cellular protein networks (Olzscha et al., 2011). However, how a simple change in the expression of one protein with a naturally occurring IDR might lead to toxicity is poorly understood at the molecular level.

Yeast prions provide an ideal system for investigating this problem. Yeast prions encompass diverse proteins, unrelated except for the presence of IDRs that can stably exist in two states: a soluble relatively unstructured species or a self-perpetuating amyloid (Shorter and Lindquist, 2005). These conformational switches can alter the function of associated globular domains, changing the cellular phenotype. The self-templating properties and meiotic transmission of prion assemblies allow them to serve as cytoplasmically inherited protein-based genetic elements (Tuite and Cox, 2003; Chien et al., 2004; Shorter and Lindquist, 2005; Halfmann and Lindquist, 2010). Seven yeast prions have been well characterized (Wickner, 1994; Sondheimer and

Correspondence to Susan Lindquist: Lindquist_admin@wi.mit.edu

Abbreviations used in this paper: IDR, intrinsically disordered region; IPOD, insoluble protein deposit; JUNQ, juxtanuclear quality control compartment; SDD-AGE, semidenaturing detergent agarose gel electrophoresis; SPB, spindle pole body.

© 2012 Treusch and Lindquist This article is distributed under the terms of an Attribution-Noncommercial-Share Alike-No Mirror Sites license for the first six months after the publication date (see <http://www.rupress.org/terms>). After six months it is available under a Creative Commons License (Attribution-Noncommercial-Share Alike 3.0 Unported license, as described at <http://creativecommons.org/licenses/by-nc-sa/3.0/>).

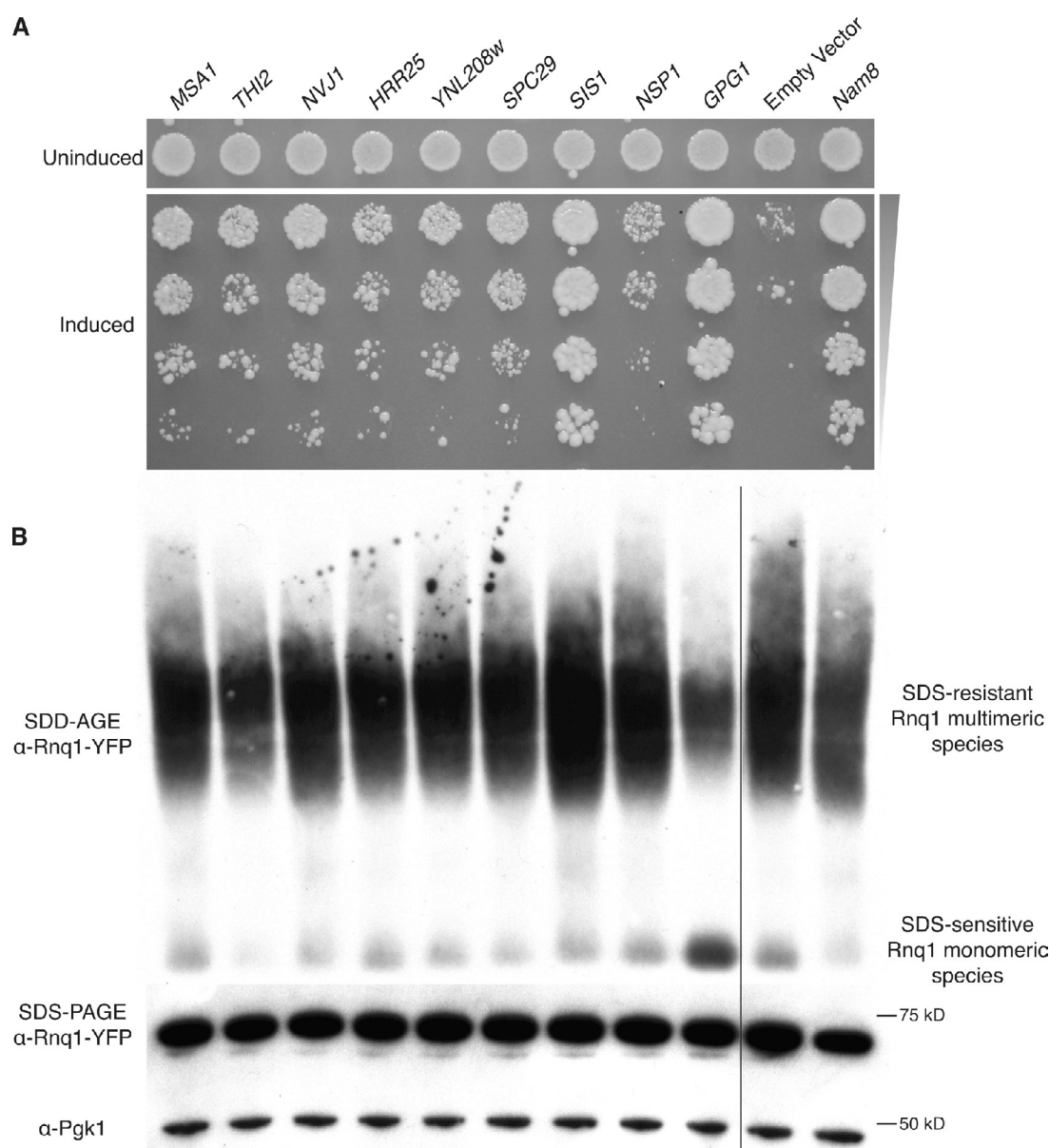


Figure 1. Suppressors of Rnq1 toxicity. (A) Strains expressing genes that suppress Rnq1 toxicity were serially diluted and spotted on a noninducing control plate and an inducing assay plate. *NAM8*, which decreases *GAL1*-mediated expression, served as a positive control for the rescue. (B) SDD-AGE analysis of the effect of overexpression screen hits on Rnq1-YFP amyloid formation. *SIS1* increased the formation of SDS-resistant Rnq1-YFP species; *GPG1* decreased it. Rnq1-YFP expression levels were examined by SDS-PAGE and Western blot analysis. Pgk1 served as a loading control. For both A and B, all samples were run on one gel, but one lane was removed (black line).

Lindquist, 2000; Du et al., 2008; Alberti et al., 2009; Brown and Lindquist, 2009; Patel et al., 2009), and ~20 other yeast proteins contain similar IDRs, prion domains, capable of forming prions (Alberti et al., 2009).

Rnq1 contains such a prion domain (Sondheimer and Lindquist, 2000). The only known biological function of Rnq1 is that its prion amyloid state, $[RNQ^+]$, facilitates the transition of other prion proteins from their soluble to their amyloid states (Derkatch et al., 2000, 2001; Osherovich and Weissman, 2001; Taneja et al., 2007). (Prions are denoted by brackets, italics, and capital letters to reflect their dominant, non-Mendelian genetic properties.) $[RNQ^+]$ also affects the conformations of other IDR-containing proteins, exemplified by its ability to induce the

glutamine-expanded exon 1 fragment of the human huntingtin protein to adopt a toxic conformation (Meriin et al., 2002).

In yeast, misfolded proteins accumulate at two distinct sites, the juxtanuclear quality control compartment (JUNQ) and the insoluble protein deposit (IPOD; Kaganovich et al., 2008). The JUNQ contains polyubiquitinated proteins targeted for proteasomal degradation. The IPOD colocalizes with the pre-autophagosomal structure at the vacuole and holds amyloidogenic proteins (Kaganovich et al., 2008; Tyedmers et al., 2010). $[RNQ^+]$ appears to influence the aggregation of other proteins through its localization to the IPOD (Kaganovich et al., 2008; Tyedmers et al., 2010). Both the JUNQ and the IPOD share features with aggresomes—highly structured protein deposits

Table 1. Categories of genes changed twofold or more upon Rnq1 overexpression

Gene expression	GO term	Cluster frequency	Background frequency	P-value	Genes
Up after 6 h	Protein folding	3/8; 37.5%	88/7,167; 1.2%	0.00201	<i>HSP104</i> , <i>SIS1</i> , and <i>SSA4</i>
Up after 8 h	Protein folding	4/23; 17.4%	88/7,167; 1.2%	0.01368	<i>HSP26</i> , <i>HSP104</i> , <i>SIS1</i> , and <i>SSA4</i>
Down after 6 h	Cytokinesis, completion of separation	4/13; 30.8%	11/7,167; 0.2%	4.90×10^{-8}	<i>CTS1</i> , <i>DSE2</i> , <i>DSE4</i> , and <i>SCW11</i>
Down after 8 h	Cytokinesis, completion of separation	5/27; 18.5%	11/7,167; 0.2%	1.98×10^{-8}	<i>CTS1</i> , <i>DSE1</i> , <i>DSE2</i> , <i>DSE4</i> , and <i>SCW11</i>
Down after 8 h	Hexose transport	3/27; 11.1%	24/7,167; 0.3%	0.00778	<i>HXT3</i> , <i>HXT6</i> , and <i>HXT7</i>

Genes that changed more than twofold in the [RNQ⁺] strain in comparison with the [rnq⁻] strain were analyzed for gene ontology (GO) term enrichment.

in higher eukaryotes that are actively formed near centrosomes (Johnston et al., 1998). But neither the JUNQ nor the IPOD associates with the spindle pole body (SPB; Kaganovich et al., 2008), and the relationship between them and aggresomes remains to be determined (Mathur et al., 2010).

Overexpression of Rnq1 is completely benign in cells whose endogenous Rnq1 is in the soluble state. But, it is specifically and extremely toxic to cells in which the endogenous Rnq1 protein has adopted the [RNQ⁺] prion amyloid state (Douglas et al., 2008). Notably, it is not excessive amyloid formation that causes toxicity. Rather, Rnq1 amyloid formation is protective. Elevated expression of Sis1, the Hsp40 co-chaperone required for Rnq1 amyloid formation (Sondheimer et al., 2001), enhances amyloid formation and concomitantly restores cell growth. Moreover, Rnq1 point mutations that decrease Sis1 interaction both increase toxicity and the formation of nonamyloid aggregates (Douglas et al., 2008). As for other proteins with IDRs, how these amorphous nonamyloid aggregates cause toxicity is unknown.

Deletion of *RNQ1* has no detectable effect on cell growth (Strawn and True, 2006). The fact that loss-of-function phenotypes are not a concern makes Rnq1 a facile model for studying the gain-of-function proteotoxicity caused by the aggregation of proteins with IDRs. Here, we investigate the molecular mechanism by which Rnq1 overexpression results in toxicity. Surprisingly, we find that elevated levels of Rnq1 cause cell cycle arrest through the highly specific sequestration of a component of the SPB.

Results and discussion

Overexpression of a diverse group of genes can suppress Rnq1 toxicity

To investigate the nature of Rnq1 toxicity, we conducted a genome-wide screen for suppressors. The screening strain carried Rnq1 in its [RNQ⁺] conformation and carried an additional copy of the *RNQ1* gene under the control of a galactose-regulated promoter. A shift of this strain from glucose to galactose medium rapidly stopped growth. The strain was mated to a strain library containing 5,532 yeast ORFs under the control of the same inducible promoter (Cooper et al., 2006; Gitler et al., 2009). Nine genes suppressed Rnq1 toxicity without having an effect on galactose-mediated gene expression: *GPG1*, *HRR25*, *MSA1*, *NSP1*, *NVJ1*, *SIS1*, *SPC29*, *THI2*, and *YNL208w* (Fig. 1 A and Table S1). The suppressors were not enriched in functional

categories, except that three are loosely connected to the cell cycle (*HRR25*, *MSA1*, and *SPC29*).

We used semidenaturing agarose gels (Bagriantsev et al., 2006; Halfmann and Lindquist, 2008) to determine whether the suppressors altered Rnq1 amyloid formation. As reported previously, Sis1 increased Rnq1 amyloid formation, whereas Gpg1 decreased it (Fig. 1 B; Douglas et al., 2008; Ishiwata et al., 2009). Other suppressors had no effect on Rnq1 formation, indicating that they modulate Rnq1 toxicity by different mechanisms.

Rnq1 toxicity results in down-regulation of cytokinetic genes

To further investigate Rnq1 toxicity, we performed microarray-based gene expression analysis. As Rnq1 overexpression is only toxic in a [RNQ⁺] background, we compared the effects of Rnq1 overexpression in isogenic strains that differed solely in the conformational status of Rnq1.

Only a few genes were differentially expressed in the [RNQ⁺] and [rnq⁻] strains (Table S2). Rnq1 overexpression resulted in the elevated transcription of several chaperones and stress-related proteins in [RNQ⁺] cells (Table 1). These included *HSP104*, *SIS1*, and *SSA4*, which are known to influence yeast prion amyloid formation. Rnq1 overexpression did not, however, trigger a general heat shock response.

GPG1, one of our screen hits, was also up-regulated, as was *BTN2* (Table S2). Overexpressed Btn2 counteracts the inheritance of the [URE3] prion and colocalizes with both Sup35 and Rnq1 prion deposits (Kryndushkin et al., 2008). Intriguingly, *BTN2* and *GPG1* expression patterns correlate with those of chaperones involved in protein folding (*BTN2*, 7.72×10^{-8}) and with the response to temperature stimulus (*GPG1*, 7.16×10^{-4} ; Hibbs et al., 2007). Thus, the up-regulation of both *BTN2* and *GPG1* may represent a previously uncharacterized cellular response to specific types of proteotoxicity.

While the genes up-regulated because of Rnq1 toxicity indicated a response to proteotoxicity, down-regulated transcripts were strongly enriched for genes involved in cytokinesis. This enrichment, together with the aforementioned genetic analysis, suggests that Rnq1 overexpression might cause a cell cycle defect (Table 1).

Rnq1 overexpression causes cell cycle arrest in mitosis

Indeed, Rnq1 overexpression for 8 h in the [RNQ⁺] background resulted in the accumulation of large-budded cells (Fig. 2 A),

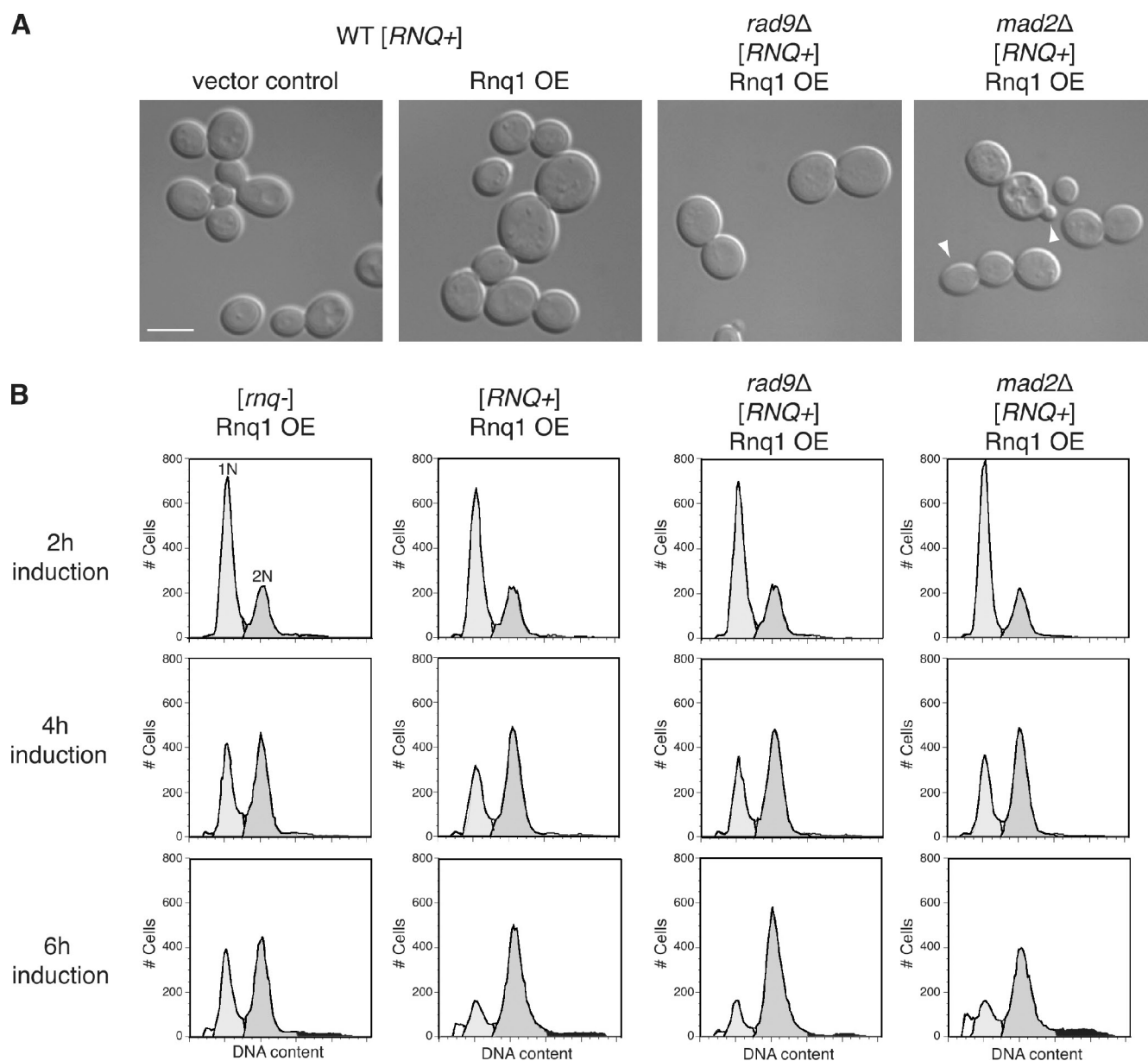


Figure 2. Rnq1 overexpression induces a MAD2-dependent cell cycle arrest. (A) Rnq1 overexpression in a [*RNQ+*] background resulted in cell cycle arrest. Deletion of *RAD9*, a component of the DNA damage checkpoint, had no effect on the arrest. On the contrary, deletion of *MAD2*, a component of the spindle checkpoint, enabled cells to rebud. Arrowheads indicate rebudded cells. Bar, 2.5 μ m. (B) Cell cycle profiles revealed that Rnq1 toxicity coincided with an increase in cells with 2N DNA content beginning at 4 h after induction. In the *mad2Δ* samples, the right-hand shoulder of the 2N peak was considerably extended at 6 h (shaded in black), indicating cells that rebudded and initiated DNA synthesis without cytokinesis. OE, overexpression; WT, wild type.

indicative of a cell cycle arrest (Hardwick, 1998; Nyberg et al., 2002). To better define the arrest point, we measured DNA content by flow cytometry. Switching midlog cultures from non-inducing raffinose to inducing galactose media initially caused a partial accumulation of cells in G1, as they adjusted to the new carbon source. Cultures of [*rnq-*] cells then returned to the normal distribution of 1N and 2N cells. [*RNQ+*] cultures, in contrast, became enriched in cells with 2N DNA content, indicating the accumulation of cells that had replicated their DNA but had not undergone mitosis (Fig. 2 B and Table S3).

A large-budded cell cycle arrest with a 2N DNA content can be triggered by the DNA damage checkpoint or the spindle checkpoint. To determine whether either contributed to the Rnq1-induced arrest, we examined cells deleted for either a critical component of the DNA damage checkpoint, *rad9Δ* (Weinert and Hartwell, 1988), or the spindle checkpoint, *mad2Δ* (Hardwick et al., 1999). Deletion of these genes alone has no effect on cell cycle progression. The *rad9Δ* deletion had no effect on Rnq1-overexpressing cells, but the *mad2Δ* deletion increased the number of cells with DNA content higher than 2N

(Fig. 2 B, black shaded areas), indicating that arrested cells rebudded and initiated further rounds of DNA synthesis without cytokinesis. By microscopy, many *mad2Δ* cells that had arrested upon Rnq1 overexpression rebudded (22.4%, SD = 2.7). In wild-type [*RNQ*⁺] cultures, only a few did (8.6%, SD = 2.6). Thus, Rnq1 overexpression triggers the spindle checkpoint, causing cell cycle arrest.

Rnq1 toxicity results in arrest with a monopolar spindle

Next, we assessed spindle formation by immunostaining for tubulin. [*rnq*[−]] cells overexpressing Rnq1 displayed the normal range of spindle morphologies expected for dividing cells (Fig. 3 A). Of [*rnq*[−]] cells, 84.7% contained short G1/S spindles, and 15.3% contained elongated metaphase/anaphase spindles. In contrast, arrested [*RNQ*⁺] cells showed an aster of microtubules proximal to the bud neck (Fig. 3 A), indicative of cells arrested with a monopolar spindle. Of [*RNQ*⁺] cells, 46.1% contained short G1/S spindles, 4.3% had long metaphase/anaphase spindles, and 49.6% displayed monopolar spindles (≥400 cells were assessed for [*rnq*[−]] and [*RNQ*⁺]).

The SPB is the microtubule organizing center, the budding yeast equivalent of the centrosome. A monopolar spindle can be caused by either a defect in SPB duplication or a failure in SPB separation after duplication. Duplication occurs early in the cell cycle, but defects in duplication or separation are not detected until the absence of a functional bipolar spindle triggers the spindle checkpoint (Jaspersen and Winey, 2004).

We used electron microscopy to determine whether cells arresting with monopolar spindles had a failure in SPB duplication or separation. Samples were prepared using cryofixation by high pressure freezing followed by freeze substitution to accurately preserve the shape and position of the SPBs (Muller et al., 2005). [*rnq*[−]] cells overexpressing Rnq1 had normal elongated spindles (Fig. 3 B). In contrast, [*RNQ*⁺] cells contained microtubule asters that originated from a single unduplicated SPB (Fig. 3 B). We examined serial thin sections of 20 arrested cells and detected no incomplete or aberrant SPBs. The morphologies of the unduplicated SPBs were similar to those previously observed with temperature-sensitive mutants of SPB components (Fig. 3 C; Donaldson and Kilmartin, 1996). Thus, in [*RNQ*⁺] cells, overexpressed Rnq1 specifically impedes duplication of the SPB.

Rnq1 overexpression causes mislocalization of Spc42

Does the defect in SPB duplication arise from aggregated forms of Rnq1 localizing to the SPB and sterically impeding its duplication? Or, might this intrinsically disordered prion selectively sequester SPB components required for duplication? Architecturally, the SPB consists of three plaques: an outer plaque facing the cytoplasm, a central plaque spanning the nuclear membrane, and an inner plaque facing the nucleoplasm (Jaspersen and Winey, 2004). We examined the colocalization of SPB components belonging to each of these structural elements with Rnq1. We used strains carrying an mCherry-tagged Rnq1 construct and endogenous SPB components tagged with GFP (Howson et al., 2005). We used the SPB components Cnm67, Nud1, and Spc72

(outer plaque); Spc97 (inner and outer); Spc110 (inner plaque); and Spc29 and Spc42 (central plaque; Jaspersen and Winey, 2004).

In [*rnq*[−]] cells that overexpressed Rnq1, all these proteins localized to two bright foci in budded cells, representing the properly duplicated SPBs. In contrast, in arrested [*RNQ*⁺] cells, most of the SPB components localized to a single focus, the unduplicated SPB (Fig. 4 A, Spc29, Spc42, Spc72, and Spc97 are shown). Uniquely, Spc42 localized both to the unduplicated SPB and to a fainter deposit within the mother cell. Notably, these faint deposits colocalized with the inclusions formed by Rnq1 at the IPOD (Fig. 4 A).

Spc42 is a highly phosphorylated coiled-coil protein that is assembled into a crystal-like structure at the core of the SPB (Bullitt et al., 1997). Interestingly, the macrostructure of Spc42 is reminiscent of the highly organized structure of amyloid fibers. Hence, we asked whether the interaction of Rnq1 and Spc42 is based on an amyloid interaction. To do so, we took advantage of the Rnq1 L94A mutant, which can induce toxicity in the absence of the [*RNQ*⁺] prion and amyloid formation (Douglas et al., 2008). This mutant induced cell cycle arrest and Spc42 mislocalization even in an [*rnq*[−]] background (Fig. 4 C). Hence, it is the nonamyloid assemblies of this IDR-containing protein that cause cytotoxicity by sequestering Spc42.

Elevated expression of Spc42 suppresses Rnq1 toxicity

If sequestration of Spc42 is the root cause of Rnq1 toxicity, elevated expression of Spc42 should counteract Rnq1 toxicity. Notably, *SPC42* was not part of the library used in our initial screen. Furthermore, expression of Spc42 from the strong *GAL1* promoter is itself toxic (Donaldson and Kilmartin, 1996). We therefore placed *SPC42* and other SBP components under the control of the constitutive *SUP35* promoter to provide more moderate overexpression. SPB components Spc72 and Spc97 had no effect, but expression of Spc42 strongly suppressed toxicity (Fig. 4). In addition, the screen hit Spc29 had a modest effect. Spc29 directly interacts with Spc42 and is thought to recruit Spc42 during SPB duplication (Adams and Kilmartin, 1999; Elliott et al., 1999). Spc29 overexpression likely counteracts the ability of Rnq1 to misdirect Spc42 by interacting with it at its proper localization.

The mislocalization of Spc42 elicited by Rnq1 overexpression provides a logical explanation for the Rnq1-induced defect in SPB duplication and the activation of the Mad2 spindle checkpoint. Indeed, the morphologies of the unduplicated SPBs in Rnq1-arrested cells were similar to those seen in cells with *SPC42* mutations (Fig. 3 C; Donaldson and Kilmartin, 1996).

Conclusions

We have taken advantage of a variety of cell biological and genetic tools available in *Saccharomyces cerevisiae* to investigate the toxicity elicited by a protein containing an IDR, the prion Rnq1. Rnq1 overexpression is profoundly toxic in cells carrying the [*RNQ*⁺] prion but not in cells with Rnq1 in its nonprion state (Douglas et al., 2008). Furthermore, Rnq1 is completely dispensable for normal growth (Strawn and True, 2006). Thus, Rnq1 affords the opportunity to analyze the toxic gain-of-function

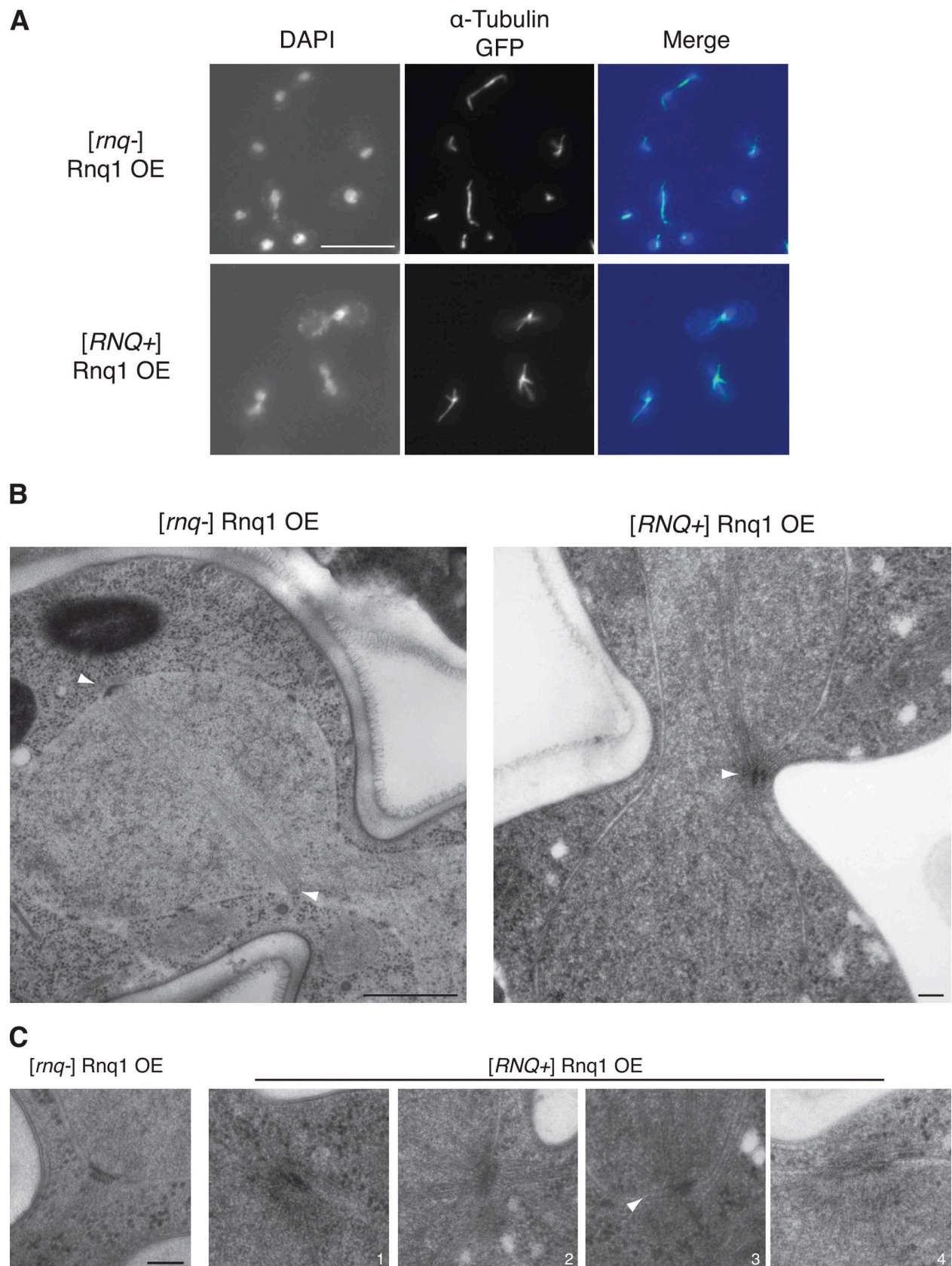


Figure 3. Rnq1 toxicity results in arrest with a monopolar spindle. (A) Tubulin immunostaining of cells overexpressing Rnq1 revealed that *[RNQ⁺]* cells arrested with a monopolar spindle. (B) Electron microscopy of cryofixed yeast showed that *[RNQ⁺]* cells arrested with an unduplicated SPB. Arrowheads indicate SPBs. (C) The unduplicated SPBs in arrested *[RNQ⁺]* cells exhibited a range of abnormal morphologies. The SPBs lacked solid central plaques and often had reduced outer plaques (1 and 2). Some arrested SPBs presented with long half-bridges (3, half-bridge indicated by the arrowhead) or had a bilobed morphology (4). OE, overexpression. Bars: (A) 5 μ m; (B, left) 500 nm; (B [right]) and (C) 100 nm.

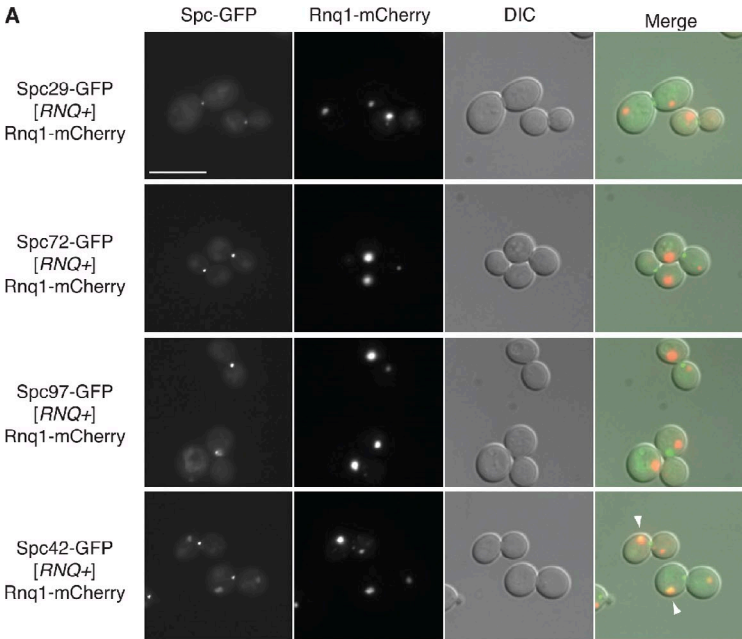
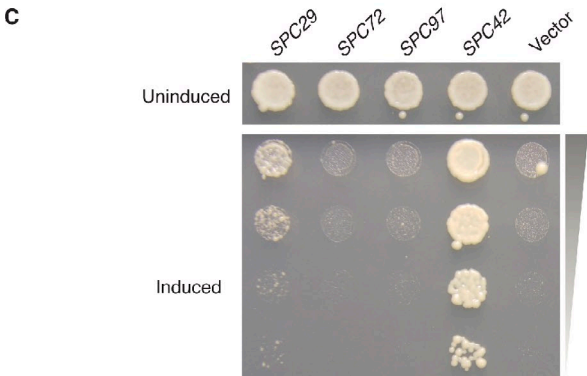
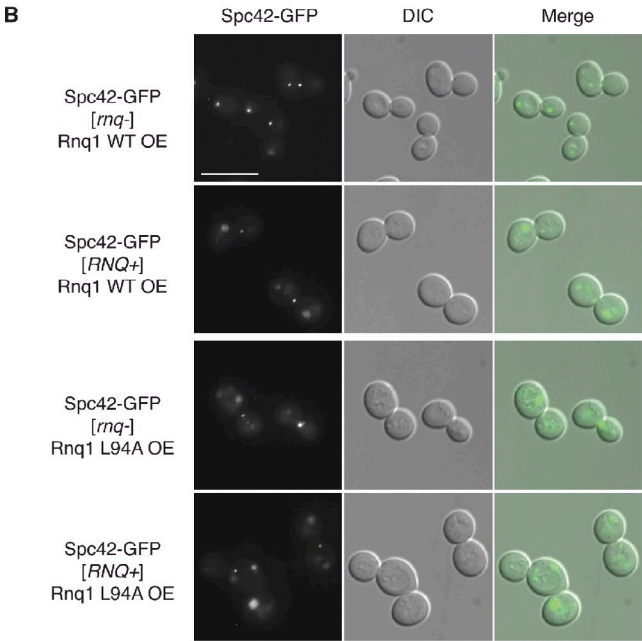


Figure 4. Rnq1 overexpression induces mislocalization of Spc42 to inclusions. (A) Rnq1 toxicity resulted in faint Spc42-GFP inclusions that colocalized with Rnq1-mCherry deposits (arrowheads). Other spindle body components did not colocalize with Rnq1. (B) In contrast to Rnq1 wild type (WT), the Rnq1 L94A mutant is toxic and forms nonamyloid aggregates in [*rnq*[−]] cells. The Rnq1 L94A mutant caused Spc42 mislocalization and cell cycle arrest in both [*rnq*[−]] and [*RNQ*⁺] cells, indicating that the interaction of Rnq1 and Spc42 is not amyloid based. (C) Moderate overexpression of Spc42 strongly suppressed Rnq1 toxicity. Spc72 and Spc97 had no effect. Spc29, an overexpression (OE) screen hit, partially suppressed toxicity. DIC, difference interference contrast. Bars, 5 μ m.



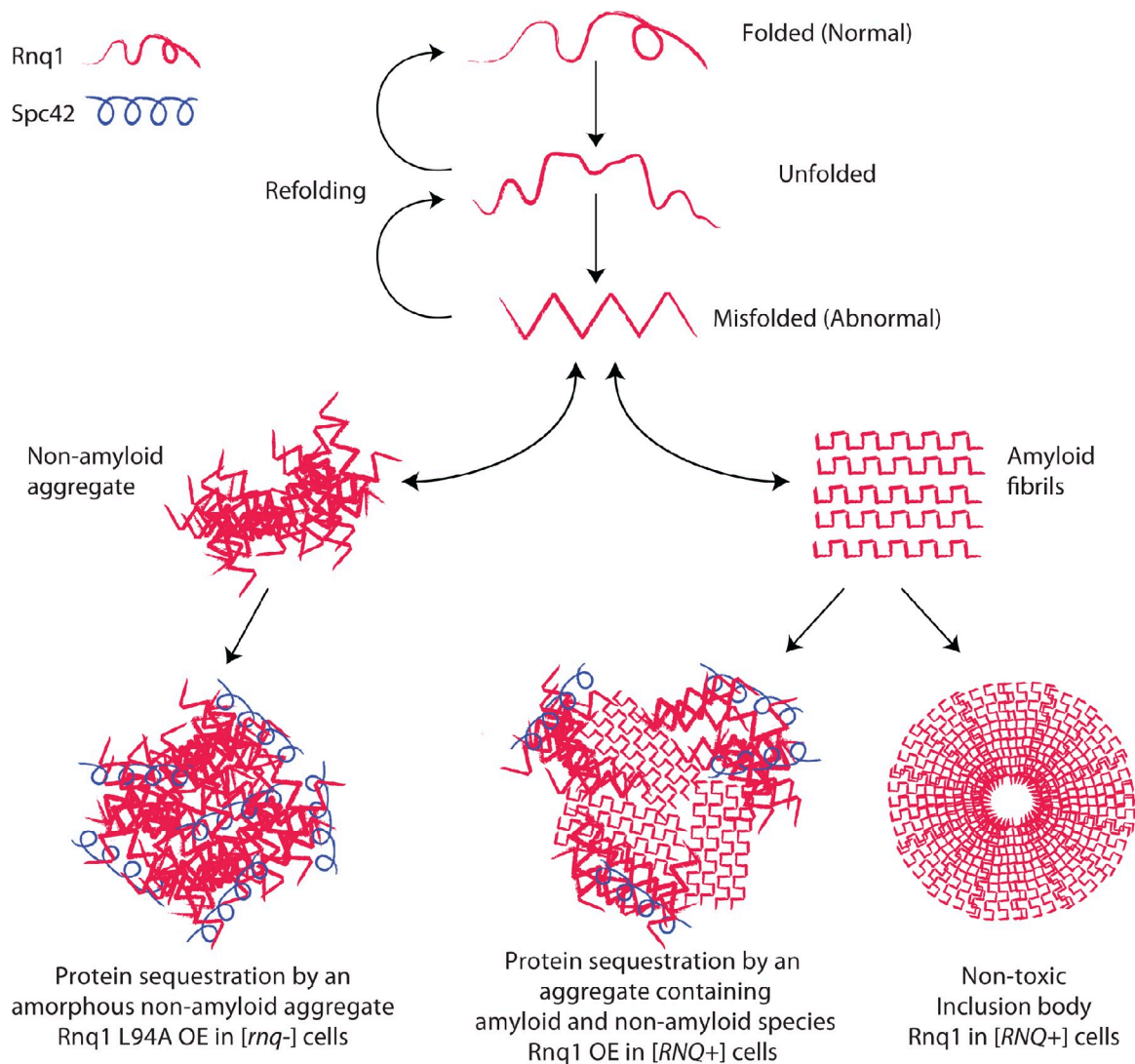


Figure 5. **Model of Rnq1 toxicity.** As an intrinsically disordered protein, Rnq1 transitions between folded, unfolded, and misfolded protein conformations. In the presence of *[RNQ⁺]* prion seeds, Rnq1 adopts the templated amyloid conformation. Overexpression (OE) of Rnq1 exceeding the capacity for amyloid formation results in the formation of nonamyloid aggregates capable of sequestering Spc42 away from its proper localization at the SPB.

interactions of an amyloidogenic protein without the loss-of-function toxicities that confound the study of other such proteins. Partial induction of the heat shock response by Rnq1 overexpression initially pointed to a general proteotoxic stress. But, further analysis established that the root cause of toxicity was the highly selective, Rnq1-mediated sequestration of the SPB protein Spc42 (Fig. 5). Rnq1 overexpression hence resulted in defective SPB duplication and cell cycle arrest. Moderate overexpression of Spc42 counteracted the defect induced by Rnq1.

The effect of Rnq1 on Spc42 is surprisingly specific. Disordered and amyloidogenic proteins have been shown to aberrantly interact with and to sequester other proteins. Intrinsically disordered proteins are likely to be toxic because of their propensity to interact promiscuously with other proteins (Vavouri et al., 2009) and, as such, to disturb cellular protein networks (Olzscha et al., 2011). For example, the toxicity of polyglutamine-expanded huntingtin (the cause of Huntington's disease) has been linked to its interactions with the transcriptional coactivator

CREB-binding protein and glyceraldehyde-3-phosphate dehydrogenase (Nucifora et al., 2001; Wu et al., 2007). Our work establishes that there are multiple ways to detoxify proteins with IDRs. As increased levels of Spc42 counteracted the effects of Rnq1-mediated sequestration, alleviating the effect of specific illicit protein interactions can ameliorate toxicity. Furthermore, either decreasing aggregation or increasing amyloid formation can detoxify IDRs. Gpg1 and Sis1 detoxify Rnq1 by these opposing mechanisms. Similarly, both decreasing and increasing amyloid formation can alleviate A β 1–42 toxicity in *Caenorhabditis elegans* (Cohen et al., 2006).

The formation of ordered inclusions appears to represent the last line in the cellular defense against proteotoxicity. Inclusions, such as aggresomes, form once proteasomal capacity has been exceeded (Johnston et al., 1998; Kaganovich et al., 2008). Aggresomes are actively formed near centrosomes (Johnston et al., 1998). Inclusion body formation serves to “sweep” the cytoplasm of potentially toxic protein species (Kopito, 2000)

and may facilitate the asymmetric inheritance of protein damage during cell division (Rujano et al., 2006; Fuentealba et al., 2008).

In yeast, misfolded proteins accumulate at two distinct sites, the JUNQ and the IPOD (Kaganovich et al., 2008). Especially, the IPOD has been likened to aggresomes, as the actin cytoskeleton mediates targeting to this structure (Ganusova et al., 2006) and as it plays a role in the asymmetric inheritance of aggregated proteins (Kryndushkin et al., 2008; Tyedmers et al., 2010). Yet, aggresomes form near centrosomes. Although a fragment of mutant huntingtin exon 1, 103QP, can colocalize with the yeast SPB and form an aggresome-like structure (Wang et al., 2009), no link between the IPOD and the SPB has been reported (Mathur et al., 2010). Rnq1 affects targeting of amyloidogenic and damaged proteins to the IPOD (Derkatch et al., 2000; Tyedmers et al., 2010), and we show that Rnq1 can also direct a core SPB component to this site. Our findings demonstrate that overexpression of a protein with an IDR can result in highly specific cellular toxicity. They also uncover a novel connection between centrosome-associated aggresomes and their apparent yeast equivalent, the IPOD.

Materials and methods

Strains and plasmids

W303 (MAT α and α can1-100, ade2-1, his3-11,15 leu2-3,112, ura3-1, trp1-1) and BY4741 (MAT α his3 Δ 1, leu2 Δ 0, met15 Δ 0, ura3 Δ 0) as well as strains from the GFP library (Howson et al., 2005) and strains from the deletion collection (Winzler et al., 1999) were used. The strains harbored Rnq1 in its [RNQ⁺] form, and isogenic [rnq⁻] strains were generated using guanidinium-HCl curing (Eaglestone et al., 2000). Plasmids with the *GAL1* promoter include pRS305-RNQ1, pRS305-RNQ1-YFP, pRS416-RNQ1 (wild type and L94A), pRS416-RNQ1-YFP, pRS426-RNQ1-YFP, pAG416-RNQ1-mCherry, and pBYO11 (centromeric, URA3, and ampicillin resistant) overexpression library constructs (Cooper et al., 2006). Plasmids that used the *SUP35* promoter include pAG415 constructs containing *SPC29*, *SPC42*, *SPC72*, and *SPC97*.

Overexpression library screen for suppressors of Rnq1 toxicity

The overexpression library screened contains ~5,800 full-length sequence verified yeast ORFs in the galactose-inducible Gateway expression plasmid pBYO11 (Cooper et al., 2006). The library was first transformed into a BY strain to create a library of yeast strains carrying the inducible overexpression constructs. We then mated a W303 strain carrying an integrated pRS305-RNQ1 construct to the library and selected for diploids. Their growth was examined on galactose plates inducing both the expression of the library clone and Rnq1. 62 putative suppressors were identified after 3–4 d of growth at 30°C. The effects of 20 of these suppressors were reproduced in the diploid screening and a haploid W303 strain. We eliminated hits that diminished *GAL1* induction by measuring the expression of YFP in their presence using flow cytometry. The identity of suppressors was verified by sequencing.

Semidenaturing detergent agarose gel electrophoresis (SDD-AGE)

Rnq1 assembly into SDS-resistant [RNQ⁺] prions was monitored by SDD-AGE as previously described (Halfmann and Lindquist, 2008). Cells were lysed in buffer containing 50 mM Hepes, pH 7.5, 150 mM NaCl, 2.5 mM EDTA, 1% Triton X-100, 30 mM *N*-ethylmaleimide, 1 mM PMSF, and a protease inhibitor cocktail (Roche) using glass beads. Lysates were spun clear of debris and mixed with 2× sample buffer [TAE [Tris base, acetic acid, and EDTA], 10% glycerol, 2% SDS, and bromophenol blue]. Samples were run on a 1.5% agarose gel containing TAE and 0.1% SDS in running buffer with the same concentrations of TAE and SDS. The gel was blotted onto Hybond-C membrane and then probed with α -GFP. Bands were visualized with ECL reagent.

Gene expression analysis

RNA was isolated from cultures induced for 4, 6, and 8 h according to Schmitt et al. (1990). RNA was labeled and hybridized to *S. cerevisiae*-specific

microarrays (Agilent Technologies). Genes that showed at least a twofold change in expression with a $P \leq 0.05$ are reported.

Cell cycle profiling

Freshly streaked cells were grown overnight at 30°C in synthetic media lacking uracil and containing 2% raffinose. Cells were diluted to an OD₅₀₀ of 0.2 and grown for an additional 3 h in the raffinose media. Cells were then washed, and Rnq1 expression was induced for the indicated time intervals in media lacking uracil and containing 2% galactose. After induction, cells were spun down in 15-ml screw cap tubes and resuspended in 3 ml of distilled H₂O. Cells were then prepared for DNA content analysis as previously described (Haase and Lew, 1997). The cells were fixed through the addition of 7 ml of 95% EtOH and overnight incubation at 4°C while rotating. After fixation, cells were spun down and resuspended in 5 ml of 50-mM sodium citrate, pH 7.4. Cells were spun down again, resuspended in 1 ml of 50-mM sodium citrate containing 0.25 mg/ml of boiled RNase A (QIAGEN), and incubated at 50°C for 1 h. 50 μ l of 20-mg/ml proteinase K (Invitrogen) was added before an additional 1-h incubation at 50°C. After this incubation, 1 ml of 50-mM sodium citrate containing 16 μ g/ml propidium iodide was added before cells were incubated overnight at 4°C. DNA content of these cells was measured using a flow cytometer (Calibur II; BD), and the resulting data were analyzed using FlowJo software.

Immunostaining

Strains were pregrown in raffinose media overnight and then induced in galactose media for 8 h (5 ml at an OD₅₀₀ of 0.2). Cells were prepared for staining as previously described (Kilmartin and Adams, 1984). Cells were spun down and resuspended in 1 ml of 3.7% formaldehyde (37% formaldehyde in 0.1 M KPi [potassium phosphate buffer], pH 6.4) after removal of the supernatant. Cells were fixed overnight at 4°C. After the fixation, cells were washed three times in 1 ml of 0.1-M KPi, pH 6.4, and then resuspended in 1 ml of 1.2-M sorbitol citrate buffer (1 liter: 218.6 g sorbitol, 17.40 g anhydrous K₂HPO₄, and 7 g citric acid; filter sterilized). Cells were spun down again and resuspended in 200 μ l of digestion mix (200 μ l of 1.2-M sorbitol citrate, 20 μ l Glusulase, and 2 μ l of 10-mg/ml Zymolase). Cells were incubated in the digestion mix for 45 min at 30°C. During the incubation, 5 μ l of 0.1% polylysine was added to each well of a 30-well slide (ER-212W; Thermo Fisher Scientific). After 5 min of incubation, the slides were washed with distilled water and allowed to air dry completely. Digested cells were spun down at 3,000 rpm for 3 min and gently resuspended in 1 ml sorbitol citrate. Cells were spun down again and then resuspended in a volume of sorbitol citrate dependent on cell pellet size (15–50 μ l). 5 μ l cells was added to each well and incubated for 10 min. Cells were removed from the side of the well using a vacuum tip. If the cell density was low, as revealed by light microscopy, more cells were added. The slides were then incubated in ice-cold methanol for 3 min followed by 10 s in ice-cold acetone. Acetone was shaken off, and slides were air dried. 4 μ l of a 1:200 antitubulin antibody [gift from A. Hochwagen, New York University, New York, NY] in PBS/BSA (1% BSA, 0.04 M K₂HPO₄, 0.01 M KH₂PO₄, 0.15 M NaCl, 0.1% NaN₃; for 100 ml: 1 g BSA, 4 ml of 1-M K₂HPO₄, 1 ml of 1-M KH₂PO₄, 15 ml of 1-M NaCl, 1 ml of 10% NaN₃, and sterilized water to 100 ml) was added to each well. Slides were incubated overnight at room temperature in a wet chamber. After the incubation, the antibody was removed using a vacuum tip, and each well was washed three times with PBS/BSA. Then, 4 μ l of the secondary antibody, 1:100 anti-mouse FITC, was added to each well and incubated for 2 h. Subsequently, each well was washed four times with PBS/BSA. 1 μ l DAPI mounting medium obtained from Vector Laboratories was added to each well before adding the coverslip and sealing the slide with nail polish.

Images were taken at room temperature on a microscope (Axiovert 200 M; Carl Zeiss) using a Plan Apochromat 100× objective (numerical aperture of 1.4), a camera (AxioCam MRm; Carl Zeiss), and the Axiovision acquisition software (Carl Zeiss). Final images were assembled from the different channels (GFP and DAPI) in Photoshop (Adobe). Brightness and contrast were adjusted equally for all images.

Electron microscopy

Yeast cultures were prepared for electron microscopy as described previously (Giddings et al., 2001). In brief, 5–10-ml aliquots of yeast cultures were collected by vacuum filtration and cryofixed by high pressure freezing in a high pressure freezer (HPM 010; Bal-Tec). Samples were then freeze substituted in either 0.25% glutaraldehyde and 0.1% uranyl acetate in acetone before embedding in an embedding kit (HM20; Lowicryl) or in 2%

osmium tetroxide and 0.1% uranyl acetate in acetone for embedding in Epon-Araldite resin. Serial thin sections were poststained in uranyl acetate and lead citrate and imaged in a transmission electron microscope (CM10 or CM100; Philips).

Fluorescence microscopy

Cells were pregrown in raffinose media and then induced in galactose media for 8 h. The effect of Rnq1 on the localization of Spc42-GFP, as well as other SPB components, was tested in GFP library strains (Howson et al., 2005). Colocalization of Rnq1-mCherry with SPB components was examined in the same fashion. Microscopy was conducted as described under Immunostaining.

Rescue of Rnq1 toxicity by Spc42

Spc42 rescue was assayed using BY Spc42-GFP strains harboring pRS416-RNQ1 and SPB components on a SUP35 promoter-controlled pAG415 plasmid. We observed similar rescue of Rnq1 toxicity by Spc29 and Spc42 in the BY and W303 backgrounds. Strains were grown overnight in media containing 2% glucose before fivefold serial dilutions were spotted on plates containing either 2% galactose or glucose. Plates were incubated for 2–3 d at 30°C and then photographed.

Online supplemental material

Table S1 lists the overexpression suppressors of Rnq1 toxicity and their functional annotations. Table S2 contains all the genes up- or down-regulated at least twofold upon Rnq1 toxicity. Table S3 contains the quantification of the cell cycle profile data presented in Fig. 2 B. Online supplemental material is available at <http://www.jcb.org/cgi/content/full/jcb.201108146/DC1>.

We thank Thomas Giddings, Michele Jones, and Mark Winey (University of Colorado, Boulder, CO) for performing the electron microscopy and helpful discussions. We are grateful to Iain Cheeseman and Andreas Hochwagen for many invaluable suggestions, reagents, and protocols. We also thank members of the Lindquist laboratory for helpful comments and discussions.

This work was supported by National Institutes of Health grant 5R37GM025874 (to S. Lindquist). S. Lindquist is a Howard Hughes Medical Institute Investigator.

Submitted: 24 August 2011

Accepted: 22 March 2012

References

- Adams, I.R., and J.V. Kilmartin. 1999. Localization of core spindle pole body (SPB) components during SPB duplication in *Saccharomyces cerevisiae*. *J. Cell Biol.* 145:809–823. <http://dx.doi.org/10.1083/jcb.145.4.809>
- Alberti, S., R. Halfmann, O. King, A. Kapila, and S. Lindquist. 2009. A systematic survey identifies prions and illuminates sequence features of prionogenic proteins. *Cell*. 137:146–158. <http://dx.doi.org/10.1016/j.cell.2009.02.044>
- Bagriantsev, S.N., V.V. Kushnirov, and S.W. Liebman. 2006. Analysis of amyloid aggregates using agarose gel electrophoresis. *Methods Enzymol.* 412:33–48. [http://dx.doi.org/10.1016/S0076-6879\(06\)12003-0](http://dx.doi.org/10.1016/S0076-6879(06)12003-0)
- Brown, J.C., and S. Lindquist. 2009. A heritable switch in carbon source utilization driven by an unusual yeast prion. *Genes Dev.* 23:2320–2332. <http://dx.doi.org/10.1101/gad.1839109>
- Bullitt, E., M.P. Rout, J.V. Kilmartin, and C.W. Akey. 1997. The yeast spindle pole body is assembled around a central crystal of Spc42p. *Cell*. 89:1077–1086. [http://dx.doi.org/10.1016/S0092-8674\(00\)80295-0](http://dx.doi.org/10.1016/S0092-8674(00)80295-0)
- Chien, P., J.S. Weissman, and A.H. DePace. 2004. Emerging principles of conformation-based prion inheritance. *Annu. Rev. Biochem.* 73:617–656. <http://dx.doi.org/10.1146/annurev.biochem.72.121801.161837>
- Chiti, F., and C.M. Dobson. 2006. Protein misfolding, functional amyloid, and human disease. *Annu. Rev. Biochem.* 75:333–366. <http://dx.doi.org/10.1146/annurev.biochem.75.101304.123901>
- Cohen, E., J. Bieschke, R.M. Perciavalle, J.W. Kelly, and A. Dillin. 2006. Opposing activities protect against age-onset proteotoxicity. *Science*. 313:1604–1610. <http://dx.doi.org/10.1126/science.1124646>
- Cooper, A.A., A.D. Gitler, A. Cashikar, C.M. Haynes, K.J. Hill, B. Bhullar, K. Liu, K. Xu, K.E. Strathearn, F. Liu, et al. 2006. Alpha-synuclein blocks ER-Golgi traffic and Rab1 rescues neuron loss in Parkinson's models. *Science*. 313:324–328. <http://dx.doi.org/10.1126/science.1129462>
- Derkatch, I.L., M.E. Bradley, S.V. Masse, S.P. Zadorsky, G.V. Polozkov, S.G. Inge-Vechtomov, and S.W. Liebman. 2000. Dependence and independence of [PSI(+)] and [PIN(+)] a two-prion system in yeast? *EMBO J.* 19:1942–1952. <http://dx.doi.org/10.1093/emboj/19.9.1942>
- Derkatch, I.L., M.E. Bradley, J.Y. Hong, and S.W. Liebman. 2001. Prions affect the appearance of other prions: the story of [PIN(+)]. *Cell*. 106:171–182. [http://dx.doi.org/10.1016/S0092-8674\(01\)00427-5](http://dx.doi.org/10.1016/S0092-8674(01)00427-5)
- Donaldson, A.D., and J.V. Kilmartin. 1996. Spc42p: a phosphorylated component of the *S. cerevisiae* spindle pole body (SPB) with an essential function during SPB duplication. *J. Cell Biol.* 132:887–901. <http://dx.doi.org/10.1083/jcb.132.5.887>
- Douglas, P.M., S. Treusch, H.Y. Ren, R. Halfmann, M.L. Duennwald, S. Lindquist, and D.M. Cyr. 2008. Chaperone-dependent amyloid assembly protects cells from prion toxicity. *Proc. Natl. Acad. Sci. USA*. 105:7206–7211. <http://dx.doi.org/10.1073/pnas.0802593105>
- Du, Z., K.W. Park, H. Yu, Q. Fan, and L. Li. 2008. Newly identified prion linked to the chromatin-remodeling factor Swi1 in *Saccharomyces cerevisiae*. *Nat. Genet.* 40:460–465. <http://dx.doi.org/10.1038/ng.112>
- Eaglestone, S.S., L.W. Ruddock, B.S. Cox, and M.F. Tuite. 2000. Guanidine hydrochloride blocks a critical step in the propagation of the prion-like determinant [PSI(+)] of *Saccharomyces cerevisiae*. *Proc. Natl. Acad. Sci. USA*. 97:240–244. <http://dx.doi.org/10.1073/pnas.97.1.240>
- Elliott, S., M. Knop, G. Schlenstedt, and E. Schiebel. 1999. Spc29p is a component of the Spc110p subcomplex and is essential for spindle pole body duplication. *Proc. Natl. Acad. Sci. USA*. 96:6205–6210. <http://dx.doi.org/10.1073/pnas.96.11.6205>
- Fuentealba, L.C., E. Eivers, D. Geissert, V. Taelman, and E.M. De Robertis. 2008. Asymmetric mitosis: Unequal segregation of proteins destined for degradation. *Proc. Natl. Acad. Sci. USA*. 105:7732–7737. <http://dx.doi.org/10.1073/pnas.0803027105>
- Ganusova, E.E., L.N. Ozols, S. Bhagat, G.P. Newnam, R.D. Wegrzyn, M.Y. Sherman, and Y.O. Chernoff. 2006. Modulation of prion formation, aggregation, and toxicity by the actin cytoskeleton in yeast. *Mol. Cell Biol.* 26:617–629. <http://dx.doi.org/10.1128/MCB.26.2.617-629.2006>
- Giddings, T.H. Jr., E.T. O'Toole, M. Morpheus, D.N. Mastronarde, J.R. McIntosh, and M. Winey. 2001. Using rapid freeze and freeze-substitution for the preparation of yeast cells for electron microscopy and three-dimensional analysis. *Methods Cell Biol.* 67:27–42. [http://dx.doi.org/10.1016/S0091-679X\(01\)67003-1](http://dx.doi.org/10.1016/S0091-679X(01)67003-1)
- Gitler, A.D., A. Chesi, M.L. Geddie, K.E. Strathearn, S. Hamamichi, K.J. Hill, K.A. Caldwell, G.A. Caldwell, A.A. Cooper, J.C. Rochet, and S. Lindquist. 2009. Alpha-synuclein is part of a diverse and highly conserved interaction network that includes PARK9 and manganese toxicity. *Nat. Genet.* 41:308–315. <http://dx.doi.org/10.1038/ng.300>
- Haase, S.B., and D.J. Lew. 1997. Flow cytometric analysis of DNA content in budding yeast. *Methods Enzymol.* 283:322–332. [http://dx.doi.org/10.1016/S0076-6879\(97\)83026-1](http://dx.doi.org/10.1016/S0076-6879(97)83026-1)
- Halfmann, R., and S. Lindquist. 2008. Screening for amyloid aggregation by Semi-Denaturing Detergent-Agarose Gel Electrophoresis. *J. Vis. Exp.* 17:838.
- Halfmann, R., and S. Lindquist. 2010. Epigenetics in the extreme: prions and the inheritance of environmentally acquired traits. *Science*. 330:629–632. <http://dx.doi.org/10.1126/science.1191081>
- Hardwick, K.G. 1998. The spindle checkpoint. *Trends Genet.* 14:1–4. [http://dx.doi.org/10.1016/S0168-9525\(97\)01340-1](http://dx.doi.org/10.1016/S0168-9525(97)01340-1)
- Hardwick, K.G., R. Li, C. Mistrot, R.H. Chen, P. Dann, A. Rudner, and A.W. Murray. 1999. Lesions in many different spindle components activate the spindle checkpoint in the budding yeast *Saccharomyces cerevisiae*. *Genetics*. 152:509–518.
- Hibbs, M.A., D.C. Hess, C.L. Myers, C. Huttenhower, K. Li, and O.G. Troyanskaya. 2007. Exploring the functional landscape of gene expression: directed search of large microarray compendia. *Bioinformatics*. 23:2692–2699. <http://dx.doi.org/10.1093/bioinformatics/btm403>
- Howson, R., W.K. Huh, S. Ghaemmaghami, J.V. Falvo, K. Bower, A. Belle, N. Dephoure, D.D. Wykoff, J.S. Weissman, and E.K. O'Shea. 2005. Construction, verification and experimental use of two epitope-tagged collections of budding yeast strains. *Comp. Funct. Genomics*. 6:2–16. <http://dx.doi.org/10.1002/cfg.449>
- Ishiwata, M., H. Kurahashi, and Y. Nakamura. 2009. A G-protein gamma subunit mimic is a general antagonist of prion propagation in *Saccharomyces cerevisiae*. *Proc. Natl. Acad. Sci. USA*. 106:791–796. <http://dx.doi.org/10.1073/pnas.0808383106>
- Jaspersen, S.L., and M. Winey. 2004. The budding yeast spindle pole body: structure, duplication, and function. *Annu. Rev. Cell Dev. Biol.* 20:1–28. <http://dx.doi.org/10.1146/annurev.cellbio.20.022003.114106>
- Johnston, J.A., C.L. Ward, and R.R. Kopito. 1998. Aggresomes: a cellular response to misfolded proteins. *J. Cell Biol.* 143:1883–1898. <http://dx.doi.org/10.1083/jcb.143.7.1883>
- Kaganovich, D., R. Kopito, and J. Frydman. 2008. Misfolded proteins partition between two distinct quality control compartments. *Nature*. 454:1088–1095. <http://dx.doi.org/10.1038/nature07195>

- Kayed, R., E. Head, J.L. Thompson, T.M. McIntire, S.C. Milton, C.W. Cotman, and C.G. Glabe. 2003. Common structure of soluble amyloid oligomers implies common mechanism of pathogenesis. *Science*. 300:486–489. <http://dx.doi.org/10.1126/science.1079469>
- Kilmartin, J.V., and A.E. Adams. 1984. Structural rearrangements of tubulin and actin during the cell cycle of the yeast *Saccharomyces*. *J. Cell Biol.* 98:922–933. <http://dx.doi.org/10.1083/jcb.98.3.922>
- Kopito, R.R. 2000. Aggresomes, inclusion bodies and protein aggregation. *Trends Cell Biol.* 10:524–530. [http://dx.doi.org/10.1016/S0962-8924\(00\)01852-3](http://dx.doi.org/10.1016/S0962-8924(00)01852-3)
- Kryndushkin, D.S., F. Shewmaker, and R.B. Wickner. 2008. Curing of the [URE3] prion by Btn2p, a Batten disease-related protein. *EMBO J.* 27:2725–2735. <http://dx.doi.org/10.1038/emboj.2008.198>
- Mathur, V., V. Taneja, Y. Sun, and S.W. Liebman. 2010. Analyzing the birth and propagation of two distinct prions, [PSI⁺] and [Het-s](y), in yeast. *Mol. Biol. Cell.* 21:1449–1461. <http://dx.doi.org/10.1091/mbc.E09-11-0927>
- Meriin, A.B., X. Zhang, X. He, G.P. Newnam, Y.O. Chernoff, and M.Y. Sherman. 2002. Huntington toxicity in yeast model depends on polyglutamine aggregation mediated by a prion-like protein Rnq1. *J. Cell Biol.* 157:997–1004. <http://dx.doi.org/10.1083/jcb.200112104>
- Muller, E.G., B.E. Snyderman, I. Novik, D.W. Hailey, D.R. Gestaut, C.A. Niemann, E.T. O'Toole, T.H. Giddings Jr., B.A. Sundin, and T.N. Davis. 2005. The organization of the core proteins of the yeast spindle pole body. *Mol. Biol. Cell.* 16:3341–3352. <http://dx.doi.org/10.1091/mbc.E05-03-0214>
- Nucifora, F.C. Jr., M. Sasaki, M.F. Peters, H. Huang, J.K. Cooper, M. Yamada, H. Takahashi, S. Tsuji, J. Troncoso, V.L. Dawson, et al. 2001. Interference by huntingtin and atrophin-1 with cbp-mediated transcription leading to cellular toxicity. *Science*. 291:2423–2428. <http://dx.doi.org/10.1126/science.1056784>
- Nyberg, K.A., R.J. Michelson, C.W. Putnam, and T.A. Weinert. 2002. Toward maintaining the genome: DNA damage and replication checkpoints. *Annu. Rev. Genet.* 36:617–656. <http://dx.doi.org/10.1146/annurev.genet.36.060402.113540>
- Olzscha, H., S.M. Schermann, A.C. Woerner, S. Pinkert, M.H. Hecht, G.G. Tartaglia, M. Vendruscolo, M. Hayer-Hartl, F.U. Hartl, and R.M. Vabulas. 2011. Amyloid-like aggregates sequester numerous metastable proteins with essential cellular functions. *Cell*. 144:67–78. <http://dx.doi.org/10.1016/j.cell.2010.11.050>
- Osherovich, L.Z., and J.S. Weissman. 2001. Multiple Gln/Asn-rich prion domains confer susceptibility to induction of the yeast [PSI⁺] prion. *Cell*. 106:183–194. [http://dx.doi.org/10.1016/S0092-8674\(01\)00440-8](http://dx.doi.org/10.1016/S0092-8674(01)00440-8)
- Patel, B.K., J. Gavin-Smyth, and S.W. Liebman. 2009. The yeast global transcriptional co-repressor protein Cyc8 can propagate as a prion. *Nat. Cell Biol.* 11:344–349. <http://dx.doi.org/10.1038/ncb1843>
- Ross, C.A., and M.A. Poirier. 2005. Opinion: What is the role of protein aggregation in neurodegeneration? *Nat. Rev. Mol. Cell Biol.* 6:891–898. <http://dx.doi.org/10.1038/nrm1742>
- Rujano, M.A., F. Bosveld, F.A. Salomons, F. Dijk, M.A. van Waarde, J.J. van der Want, R.A. de Vos, E.R. Brunt, O.C. Sibon, and H.H. Kampinga. 2006. Polarised asymmetric inheritance of accumulated protein damage in higher eukaryotes. *PLoS Biol.* 4:e417. <http://dx.doi.org/10.1371/journal.pbio.0040417>
- Schmitt, M.E., T.A. Brown, and B.L. Trumpower. 1990. A rapid and simple method for preparation of RNA from *Saccharomyces cerevisiae*. *Nucleic Acids Res.* 18:3091–3092. <http://dx.doi.org/10.1093/nar/18.10.3091>
- Shorter, J., and S. Lindquist. 2005. Prions as adaptive conduits of memory and inheritance. *Nat. Rev. Genet.* 6:435–450. <http://dx.doi.org/10.1038/nrg1616>
- Sondheimer, N., and S. Lindquist. 2000. Rnq1: an epigenetic modifier of protein function in yeast. *Mol. Cell.* 5:163–172. [http://dx.doi.org/10.1016/S1097-2765\(00\)80412-8](http://dx.doi.org/10.1016/S1097-2765(00)80412-8)
- Sondheimer, N., N. Lopez, E.A. Craig, and S. Lindquist. 2001. The role of Sis1 in the maintenance of the [RNQ⁺] prion. *EMBO J.* 20:2435–2442. <http://dx.doi.org/10.1093/emboj/20.10.2435>
- Stefani, M., and C.M. Dobson. 2003. Protein aggregation and aggregate toxicity: new insights into protein folding, misfolding diseases and biological evolution. *J. Mol. Med.* 81:678–699. <http://dx.doi.org/10.1007/s00109-003-0464-5>
- Strawn, L.A., and H.L. True. 2006. Deletion of RNQ1 gene reveals novel functional relationship between divergently transcribed Bik1p/CLIP-170 and Sfi1p in spindle pole body separation. *Curr. Genet.* 50:347–366. <http://dx.doi.org/10.1007/s00294-006-0098-6>
- Taneja, V., M.L. Maddelein, N. Talarek, S.J. Saupe, and S.W. Liebman. 2007. A non-Q/N-rich prion domain of a foreign prion, [Het-s], can propagate as a prion in yeast. *Mol. Cell.* 27:67–77. <http://dx.doi.org/10.1016/j.molcel.2007.05.027>
- Treusch, S., D.M. Cyr, and S. Lindquist. 2009. Amyloid deposits: protection against toxic protein species? *Cell Cycle*. 8:1668–1674. <http://dx.doi.org/10.4161/cc.8.11.8503>
- Tuite, M.F., and B.S. Cox. 2003. Propagation of yeast prions. *Nat. Rev. Mol. Cell Biol.* 4:878–890. <http://dx.doi.org/10.1038/nrm1247>
- Tyedmers, J., S. Treusch, J. Dong, J.M. McCaffery, B. Bevis, and S. Lindquist. 2010. Prion induction involves an ancient system for the sequestration of aggregated proteins and heritable changes in prion fragmentation. *Proc. Natl. Acad. Sci. USA*. 107:8633–8638. <http://dx.doi.org/10.1073/pnas.1003895107>
- Vavouri, T., J.I. Semple, R. Garcia-Verdugo, and B. Lehner. 2009. Intrinsic protein disorder and interaction promiscuity are widely associated with dosage sensitivity. *Cell*. 138:198–208. <http://dx.doi.org/10.1016/j.cell.2009.04.029>
- Wang, Y., A.B. Meriin, N. Zaarur, N.V. Romanova, Y.O. Chernoff, C.E. Costello, and M.Y. Sherman. 2009. Abnormal proteins can form aggresome in yeast: aggresome-targeting signals and components of the machinery. *FASEB J.* 23:451–463. <http://dx.doi.org/10.1096/fj.08-117614>
- Weinert, T.A., and L.H. Hartwell. 1988. The RAD9 gene controls the cell cycle response to DNA damage in *Saccharomyces cerevisiae*. *Science*. 241:317–322. <http://dx.doi.org/10.1126/science.3291120>
- Wickner, R.B. 1994. [URE3] as an altered URE2 protein: evidence for a prion analog in *Saccharomyces cerevisiae*. *Science*. 264:566–569. <http://dx.doi.org/10.1126/science.7909170>
- Winzler, E.A., D.D. Shoemaker, A. Astromoff, H. Liang, K. Anderson, B. Andre, R. Bangham, R. Benito, J.D. Boeke, H. Bussey, et al. 1999. Functional characterization of the *S. cerevisiae* genome by gene deletion and parallel analysis. *Science*. 285:901–906. <http://dx.doi.org/10.1126/science.285.5429.901>
- Wu, J., F. Lin, and Z. Qin. 2007. Sequestration of glyceraldehyde-3-phosphate dehydrogenase to aggregates formed by mutant huntingtin. *Acta Biochim. Biophys. Sin. (Shanghai)*. 39:885–890. <http://dx.doi.org/10.1111/j.1745-7270.2007.00352.x>

Supplemental material

JCB

Treusch and Lindquist, <http://www.jcb.org/cgi/content/full/jcb.201108146/DC1>

Table S1. Suppressors of Rnq1 toxicity identified in the overexpression screen

Standard name	Functional annotations
<i>GPG1</i>	Proposed γ subunit of the heterotrimeric G protein; overproduction causes prion curing
<i>HRR25</i>	Protein kinase involved in regulating diverse events, including vesicular trafficking, DNA repair, and chromosome segregation
<i>MSA1</i>	Activator of G1-specific transcription factors, involved in regulation of the timing of cell cycle initiation
<i>NSP1</i>	Essential component of the nuclear pore complex, which mediates nuclear import and export
<i>NVJ1</i>	Nuclear envelope protein, involved in nuclear microautophagy
<i>SIS1</i>	Type II HSP40 co-chaperone that interacts with the HSP70 protein Ssa1p
<i>SPC29</i>	Inner plaque SPB component, required for SPB duplication
<i>THI2</i>	Zinc finger protein of the Zn(II)2Cys6 type; probable transcriptional activator of thiamine biosynthetic genes
<i>YNL208w</i>	Protein of unknown function

Functional annotations are based on the *Saccharomyces* Genome Database.

Table S2. Genes up- or down-regulated upon Rnq1 overexpression

Gene expression	Genes
Up after 6 h	<i>ARG1</i> , <i>FMP16</i> , <i>HSP104</i> , <i>MBF1</i> , <i>SIS1</i> , <i>SSA4</i> , <i>YDL038C</i> , and <i>YGP1</i>
Down after 6 h	<i>ALD4</i> , <i>CRP1</i> , <i>CTS1</i> , <i>DSE2</i> , <i>DSE4</i> , <i>EGT2</i> , <i>GSY2</i> , <i>HO</i> , <i>HPF1</i> , <i>PHO84</i> , <i>PRY3</i> , <i>REE1</i> , and <i>SCW11</i>
Up after 8 h	<i>BTN2</i> , <i>DBF2</i> , <i>FBP1</i> , <i>FMP16</i> , <i>GND2</i> , <i>GPG1</i> , <i>HSP104</i> , <i>HSP12</i> , <i>HSP26</i> , <i>IDP2</i> , <i>MBF1</i> , <i>NCA3</i> , <i>PCK1</i> , <i>PIR3</i> , <i>RPL32</i> , <i>SFC1</i> , <i>SIS1</i> , <i>SSA4</i> , <i>YGP1</i> , <i>YJL144W</i> , <i>YLR040C</i> , <i>YPS3</i> , and <i>YRO2</i>
Down after 8 h	<i>ALD4</i> , <i>CTS1</i> , <i>DSE1</i> , <i>DSE2</i> , <i>DSE4</i> , <i>EGT2</i> , <i>FET3</i> , <i>FIT2</i> , <i>GSY1</i> , <i>HTA2</i> , <i>HXT3</i> , <i>HXT6</i> , <i>HXT7</i> , <i>INO1</i> , <i>LSP1</i> , <i>MRP1</i> , <i>PDH1</i> , <i>PHO84</i> , <i>PLB2</i> , <i>PRY3</i> , <i>PSA1</i> , <i>RGI1</i> , <i>SCW11</i> , <i>SIM1</i> , <i>SIT1</i> , <i>SUN4</i> , and <i>YDR133C</i>

Rnq1 was overexpressed in [*rnq*⁻] and [*RNQ*⁺] strains. Shown are genes that changed at least twofold in the [*RNQ*⁺] strain in comparison with the [*rnq*⁻] strain. Genes are grouped by time point and directionality of the change in their expression. We also measured gene expression after 4 h of Rnq1 overexpression, but at that point, we found no significant differences in gene expression.

Table S3. Quantification of cell cycle profiling of a strain overexpressing Rnq1

Sample	Time of Rnq1 induction	DNA content	
		1N	2N
	<i>h</i>	%	%
[<i>rnq</i> ⁻]	0	42.1	52.6
[<i>rnq</i> ⁻]	2	66.8	30.4
[<i>rnq</i> ⁻]	4	40.8	54.5
[<i>rnq</i> ⁻]	6	38.4	54.2
[<i>RNQ</i> ⁺]	0	44.8	51.4
[<i>RNQ</i> ⁺]	2	65.7	31.3
[<i>RNQ</i> ⁺]	4	32.4	62.8
[<i>RNQ</i> ⁺]	6	19.4	69.9
<i>rad9Δ</i> [<i>RNQ</i> ⁺]	0	42.9	53.1
<i>rad9Δ</i> [<i>RNQ</i> ⁺]	2	64.9	31.9
<i>rad9Δ</i> [<i>RNQ</i> ⁺]	4	33.3	62.3
<i>rad9Δ</i> [<i>RNQ</i> ⁺]	6	16.7	77.8
<i>mad2Δ</i> [<i>RNQ</i> ⁺]	0	51.5	42.5
<i>mad2Δ</i> [<i>RNQ</i> ⁺]	2	70.5	27
<i>mad2Δ</i> [<i>RNQ</i> ⁺]	4	35.7	60.6
<i>mad2Δ</i> [<i>RNQ</i> ⁺]	6	22.1	60.6

In [*RNQ*⁺] strains, Rnq1 overexpression results in an increased number of cells with 2N DNA content. This suggests that Rnq1 overexpression results in a cell cycle arrest between S phase and G1.